Electronic Supplementary Material (ESI) for CrystEngComm.

Supplementary Information

to

Experimental Tests for Quality Validation of Computationally Predicted Crystal Structures – A Case of a Conformationally Flexible Procyanidin A2 Dihydrate

Marta K. Dudek, Grzegorz Bujacz, Marek J. Potrzebowski

Contents:

Computational details

For conformational search universal force field was used, together with ultra-fine quality settings. Simulated annealing algorithm was used to generate possible crystal structures for the selected conformers, with the following settings, corresponding to the ultra-fine quality: a temperature range of 300-1.5*10^5 K, a heating factor of 0.025, 14 consecutive steps accepted before cooling, and a maximum of 10000 steps. For the primary geometry optimization of all generated structures convergence criteria were as follows: 2*10^{-5} kcal/mol for energy, 0.001 kcal/mol/Å^3 for maximum force, and 1*10^{-5} for displacement. For subsequent DFT-D calculations of the 67 selected structures, the convergence criteria were set to medium quality, which corresponds to 2*10^{-5} eV/atom for energy tolerance, 0.05 eV/Å for maximum force, and 0.002Å for displacement tolerance. A Monkhorst–Pack grid of 2x1x1 was used to sample the Brillouin zone, with a k-points separation of 0.08Å^{-1}.

Table S1. 120 conformers obtained after conformational search for PA-2, together with the torsion angles values and energies from universal force field.

conformer	ϕ (upper unit) [°]	ψ (lower unit) [°]	total energy [eV]
1	-87	59	170.48
2	93	59	170.66
3	-57	59	170.75
4	123	59	170.95
5	-87	-121	171.03
6	93	-121	171.21
7	-57	-121	171.30
8	123	-121	171.50
9	-87	-1	172.64
10	93	-1	172.82
11	-57	-1	172.91
12	123	-1	173.11
13	-87	179	175.28
14	93	179	175.47
15	-57	179	175.55
16	153	59	175.64
17	123	179	175.76
18	-87	29	175.76
19	93	29	175.95
20	-57	29	176.03
21	153	-121	176.19
22	123	29	176.24
23	-27	59	177.09
24	-87	-31	177.26
25	93	-31	177.44
26	-57	-31	177.53
27	-27	-121	177.64
28	123	-31	177.73

29	153	-1	177.79
30	-87	149	178.40
31	93	149	178.58
32	-57	149	178.67
33	123	149	178.87
34	-27	-1	179.24
35	153	179	180.44
36	-87	-151	180.47
37	93	-151	180.65
38	-57	-151	180.74
39	153	29	180.92
40	123	-151	180.94
41	-27	179	181.89
42	-27	29	182.37
43	153	-31	182.41
44	153	149	183.56
45	-27	-31	183.87
46	-27	149	185.01
47	153	-151	185.63
48	-27	-151	187.08
49	-87	89	203.72
50	93	89	203.90
51	-57	89	203.99
52	123	89	204.19
53	153	89	208.88
54	63	59	209.86
55	-27	89	210.33
56	63	-121	210.41
57	63	-1	212.02
58	-117	59	212.28
59	-117	-121	212.83
60	-117	-1	214.44
61	63	179	214.66
62	63	29	215.14
63	63	-31	216.64
64	-117	179	217.08
65	-117	29	217.56
66	63	149	217.78
67	-117	-31	219.06
68	63	-151	219.85
69	-117	149	220.20
70	-117	-151	222.27
71	-87	-91	222.62
72	93	-91	222.80
73	-57	-91	222.89
74	123	-91	223.09
75	153	-91	227.78
76	-27	-91	229.23
77	63	89	243.10

78	-117	89	245.52
79	63	-91	262.00
80	-117	-91	264.42
81	-177	59	360.52
82	-177	-121	361.07
83	-177	-1	362.67
84	-177	179	365.32
85	-177	29	365.80
86	-177	-31	367.29
87	-177	149	368.44
88	-177	-151	370.51
89	-87	119	391.09
90	93	119	391.27
91	-57	119	391.36
92	123	119	391.56
93	3	59	392.33
94	3	-121	392.87
95	-177	89	393.76
96	3	-1	394.48
97	153	119	396.24
98	3	179	397.13
99	3	29	397.61
100	-27	119	397.69
101	3	-31	399.10
102	3	149	400.25
103	3	-151	402.31
104	-177	-91	412.66
105	3	89	425.56
106	63	119	430.47
107	-117	119	432.88
108	3	-91	444.46
109	-177	119	581.12
110	-87	-61	599.70
111	93	-61	599.88
112	-57	-61	599.97
113	123	-61	600.17
114	153	-61	604.85
115	-27	-61	606.31
116	3	119	612.93
117	63	-61	639.08
118	-117	-61	641.50
119	-177	-61	789.74
120	3	-61	821.54

Table S2. Energy and NMR rankings of the final 67 structures: rank 1 refers to results obtained with universal force field optimization, rank 2 to results obtained after PBE-TS optimization with cell parameters adjustments, rank 3 to the agreement between theoretical and experimental NMR parameters. R_{final} value refers to the NMR ranking, while ΔE is an energy difference from 2nd ranking (in eV) in reference to the most stable structure [**6**-*P*2_1(3)]

No	ϕ and ψ angels	space group	structure name	rank 1	rank 2	rank 3	R_{final}	ΔE [eV]
1	–70°; +66°	*P*1	**1**-*P*1(1)	1	32	48	0.765	2.79
		*P*1	**1**-*P*1(2)	2	35	61	0.689	2.96
		P$2_12_12_1$	**1**-*P*$2_12_12_1$(1)	3	38	24	0.804	3.14
		P$2_12_12_1$	**1**-*P*$2_12_12_1$(2)	4	34	34	0.793	2.96
		P$2_12_12_1$	**1**-*P*$2_12_12_1$(3)	5	37	28	0.801	3.03
		P$2_12_12_1$	**1**-*P*$2_12_12_1$(4)	6	61	66	0.605	4.41
		*C*2	**1**-*C*2(1)	7	14	47	0.766	1.59
		P2_1	**1**-*P*2_1(1)	10	51	25	0.803	3.63
		P2_1	**1**-*P*2_1(2)	11	62	14	0.846	4.42
2	+118°; +64°	*P*1	**2**-*P*1(1)	15	48	46	0.767	3.53
		*P*1	**2**-*P*1(2)	16	57	10	0.853	4.12
		*P*1	**2**-*P*1(3)	19	8	5	0.889	0.76
		P$2_12_12_1$	**2**-*P*$2_12_12_1$(1)	35	49	54	0.738	3.57
		*C*2	**2**-*C*2(1)	64	54	11	0.852	3.74
		*C*2	**2**-*C*2(2)	65	25	39	0.786	2.34
		*C*2	**2**-*C*2(3)	66	30	50	0.764	2.74
		P2_1	**2**-*P*2_1(1)	51	55	26	0.802	3.89
		P2_1	**2**-*P*2_1(2)	58	46	55	0.733	3.51
3	–71°; +63°	*P*1	**3**-*P*1(1)	12	43	32	0.795	3.48
		*P*1	**3**-*P*1(2)	13	20	57	0.720	1.88
		*P*1	**3**-*P*1(3)	14	50	7	0.861	3.59
		*P*1	**3**-*P*1(4)	17	47	63	0.669	3.52
		P$2_12_12_1$	**3**-*P*$2_12_12_1$(1)	44	67	33	0.795	5.41
		P$2_12_12_1$	**3**-*P*$2_12_12_1$(2)	45	5	56	0.727	0.57
		P$2_12_12_1$	**3**-*P*$2_12_12_1$(3)	49	63	22	0.816	4.60
		P$2_12_12_1$	**3**-*P*$2_12_12_1$(4)	53	31	49	0.765	2.76
		P$2_12_12_1$	**3**-*P*$2_12_12_1$(5)	54	44	65	0.607	3.49
		P$2_12_12_1$	**3**-*P*$2_12_12_1$(6)	56	45	9	0.854	3.51
		P$2_12_12_1$	**3**-*P*$2_12_12_1$(7)	57	18	51	0.762	1.71
		*C*2	**3**-*C*2(1)	46	42	19	0.824	3.43
		*C*2	**3**-*C*2(2)	50	41	16	0.831	3.37
		P2_1	**3**-*P*2_1(1)	21	59	44	0.773	4.24
		P2_1	**3**-*P*2_1(2)	22	58	12	0.852	4.15
4	+116°; +88°	*P*1	**4**-*P*1(1)	33	60	58	0.719	4.28
		*P*1	**4**-*P*1(2)	37	4	20	0.822	0.54
		P$2_12_12_1$	**4**-*P*$2_12_12_1$(1)	55	29	31	0.796	2.73
		P$2_12_12_1$	**4**-*P*$2_12_12_1$(2)	60	39	64	0.665	3.34

		*C*2	**4**-*C*2(1)	67	66	60	0.692	5.21
		$P2_1$	**4**-$P2_1$(1)	61	12	52	0.758	1.27
		$P2_1$	**4**-$P2_1$(2)	63	11	67	0.565	1.05
5	–103°; –110°	*P*1	**5**-*P*1(1)	18	53	40	0.785	3.69
		*P*1	**5**-*P*1(2)	20	56	42	0.783	3.92
		$P2_12_12_1$	**5**-$P2_12_12_1$(1)	23	21	38	0.790	1.88
		*C*2	**5**-*C*2(1)	29	33	15	0.841	2.93
		$P2_1$	**5**-$P2_1$(1)	34	6	37	0.790	0.73
		$P2_1$	**5**-$P2_1$(2)	36	52	62	0.681	3.69
		$P2_1$	**5**-$P2_1$(3)	38	19	21	0.822	1.82
		$P2_1$	**5**-$P2_1$(4)	39	26	17	0.826	2.45
		$P2_1$	**5**-$P2_1$(5)	41	9	45	0.770	0.99
		$P2_1$	**5**-$P2_1$(6)	42	28	6	0.864	2.59
		$P2_1$	**5**-$P2_1$(7)	43	65	59	0.718	5.02
6	+75°; –117°	*P*1	**6**-*P*1(1)	8	40	23	0.808	3.36
		$P2_12_12_1$	**6**-$P2_12_12_1$(1)	31	24	1	0.927	2.16
		*C*2	**6**-*C*2(1)	62	36	53	0.744	3.00
		$P2_1$	**6**-$P2_1$(1)	47	2	2	0.921	0.02
		$P2_1$	**6**-$P2_1$(2)	48	17	4	0.899	1.69
		$P2_1$	**6**-$P2_1$(3)	52	1	8	0.859	0.00
		$P2_1$	**6**-$P2_1$(4)	59	10	3	0.916	1.04
7	–104°; –107°	*P*1	**7**-*P*1(1)	9	64	13	0.848	4.84
		$P2_12_12_1$	**7**-$P2_12_12_1$(1)	26	15	27	0.801	1.65
		$P2_12_12_1$	**7**-$P2_12_12_1$(2)	27	22	30	0.798	2.08
		$P2_12_12_1$	**7**-$P2_12_12_1$(3)	32	23	43	0.780	2.05
		*C*2	**7**-*C*2(1)	40	13	41	0.785	1.40
		$P2_1$	**7**-$P2_1$(1)	24	7	35	0.792	0.61
		$P2_1$	**7**-$P2_1$(2)	25	3	29	0.800	0.42
		$P2_1$	**7**-$P2_1$(3)	28	16	36	0.791	1.66
		$P2_1$	**7**-$P2_1$(4)	30	27	18	0.825	2.46

Table S3. ^{1}H and ^{13}C solid-state NMR data (in ppm) for PA-2.

atom	$^{13}C(\delta_{iso})$	$^{13}C(\delta_{11})$	$^{13}C(\delta_{22})$	$^{13}C(\delta_{33})$	$^{1}H(\delta_{iso})$
2	102.93	157.78	133.03	25.83	-
3	65.15				4.0
4	25.00				3.6
5	154.08	240.29	158.52	70.11	-
6	96.80				5.3
7	154.08	240.29	158.52	70.11	-
8	95.20	156.7	105.21	30.44	6.1
9	152.87	242.43	158.56	64.73	-
10	96.80	164.94	121.77	12.98	-
11	128.82	216.91	150.17	23.93	-
12	112.26	185.09	130.27	28.15	6.7
13	142.61	214.76	156.59	63.07	-
14	142.61	214.76	156.59	63.07	-
15	114.50	191.91	132.66	25.21	4.6
16	121.07	210.72	153.6	4.56	5.6
2’	78.20				4.1
3’	64.40				4.4
4’	28.71				2.0; 2.4
5’	151.63	239.57	157.36	62.46	-
6’	96.80				5.3
7’	148.94	232.97	156.91	63.56	-
8’	102.16	150.46	141.87	20.15	-
9’	147.79	224.76	157.91	67.46	-
10’	97.60				-
11’	130.33	222.43	154.69	20.64	-
12’	119.25	194.71	131.49	38.74	6.5
13’	142.70	211.46	157.1	66.95	-
14’	144.30	214.56	158.45	67.93	-
15’	116.56	193.9	139.09	24.33	7.5
16’	118.77	200.47	134.13	27.84	7.1

Table S4. Correlation coefficients (R^2) derived from correlation of theoretical and experimental NMR data. For comparison purposes calculated NMR parameters for optimized X-Ray structure is given.

Structure	$^{13}C(\delta_{iso})$	$^{13}C(\delta_{11})$	$^{13}C(\delta_{22})$	$^{13}C(\delta_{33})$	$^{1}H(\delta_{iso})$
1-*P*$2_12_12_1$(1)	0.988	0.924	0.776	0.916	0.781
1-*P*$2_12_12_1$(2)	0.988	0.934	0.760	0.913	0.767
1-*P*$2_12_12_1$(3)	0.989	0.921	0.762	0.916	0.779
1-*P*$2_12_12_1$(4)	0.989	0.935	0.823	0.887	0.513
1-*C*2(1)	0.985	0.907	0.828	0.886	0.730
1-*P*1(1)	0.994	0.930	0.867	0.897	0.721
1-*P*1(2)	0.990	0.956	0.864	0.868	0.620
1-*P*2_1(1)	0.987	0.910	0.765	0.908	0.784
1-*P*2_1(2)	0.987	0.912	0.663	0.907	0.852
2-*P*$2_12_12_1$(1)	0.992	0.928	0.774	0.874	0.698
2-*C*2(1)	0.986	0.936	0.656	0.877	0.861
2-*C*2(2)	0.989	0.949	0.748	0.902	0.759
2-*C*2(3)	0.990	0.921	0.760	0.919	0.730
2-*P*1(1)	0.980	0.945	0.764	0.890	0.734
2-*P*1(2)	0.988	0.893	0.773	0.898	0.852
2-*P*1(3)	0.991	0.956	0.814	0.908	0.888
2-*P*2_1(1)	0.990	0.960	0.785	0.926	0.772
2-*P*2_1(2)	0.983	0.906	0.751	0.896	0.694
3-*P*$2_12_12_1$(1)	0.989	0.901	0.845	0.910	0.765
3-*P*$2_12_12_1$(2)	0.994	0.911	0.872	0.933	0.668
3-*P*$2_12_12_1$(3)	0.987	0.894	0.806	0.916	0.797
3-*P*$2_12_12_1$(4)	0.987	0.947	0.822	0.916	0.721
3-*P*$2_12_12_1$(5)	0.989	0.933	0.848	0.898	0.512
3-*P*$2_12_12_1$(6)	0.992	0.928	0.834	0.893	0.844
3-*P*$2_12_12_1$(7)	0.992	0.953	0.837	0.904	0.717
3-*C*2(1)	0.991	0.896	0.771	0.945	0.808
3-*C*2(2)	0.990	0.897	0.744	0.941	0.821
3-*P*1(1)	0.989	0.941	0.794	0.896	0.768
3-*P*1(2)	0.984	0.935	0.800	0.897	0.667
3-*P*1(3)	0.993	0.919	0.852	0.921	0.849
3-*P*1(4)	0.989	0.930	0.874	0.890	0.592
3-*P*2_1(1)	0.988	0.882	0.775	0.913	0.745
3-*P*2_1(2)	0.991	0.905	0.767	0.914	0.848
4-*P*$2_12_12_1$(1)	0.992	0.900	0.802	0.894	0.773
4-*P*$2_12_12_1$(2)	0.989	0.892	0.859	0.884	0.594
4-*C*2(1)	0.986	0.900	0.708	0.884	0.646
4-*P*1(1)	0.991	0.927	0.736	0.888	0.675
4-*P*1(2)	0.990	0.942	0.774	0.900	0.805
4-*P*2_1(1)	0.992	0.946	0.780	0.923	0.716
4-*P*2_1(2)	0.992	0.933	0.768	0.905	0.464
5-*P*$2_12_12_1$(1)	0.990	0.926	0.787	0.918	0.761

5-*C*2(1)	0.994	0.916	0.780	0.934	0.829
5-*P*1(1)	0.989	0.912	0.931	0.880	0.744
5-*P*1(2)	0.990	0.910	0.931	0.880	0.741
5-$P2_1$(1)	0.995	0.919	0.805	0.936	0.758
5-$P2_1$(2)	0.988	0.922	0.781	0.916	0.617
5-$P2_1$(3)	0.996	0.912	0.848	0.934	0.796
5-$P2_1$(4)	0.994	0.922	0.866	0.933	0.799
5-$P2_1$(5)	0.995	0.928	0.833	0.936	0.727
5-$P2_1$(6)	0.987	0.906	0.793	0.938	0.859
5-$P2_1$(7)	0.987	0.919	0.849	0.913	0.660
6-$P2_12_12_1$(1)	0.994	0.935	0.854	0.930	0.934
6-$P2_1$(1)	0.994	0.879	0.908	0.921	0.927
6-$P2_1$(2)	0.992	0.930	0.826	0.912	0.902
6-$P2_1$(3)	0.992	0.912	0.785	0.911	0.856
6-$P2_1$(4)	0.995	0.935	0.854	0.925	0.920
6-*C*2(1)	0.985	0.912	0.748	0.924	0.705
6-*P*1(1)	0.991	0.898	0.816	0.913	0.785
7-$P2_12_12_1$(1)	0.991	0.913	0.798	0.926	0.775
7-$P2_12_12_1$(2)	0.992	0.928	0.799	0.916	0.770
7-$P2_12_12_1$(3)	0.991	0.916	0.779	0.923	0.749
7-*C*2(1)	0.993	0.918	0.807	0.917	0.753
7-*P*1(1)	0.987	0.877	0.806	0.893	0.844
7-$P2_1$(1)	0.989	0.873	0.704	0.923	0.778
7-$P2_1$(2)	0.989	0.893	0.716	0.924	0.785
7-$P2_1$(3)	0.991	0.906	0.781	0.922	0.765
7-$P2_1$(4)	0.994	0.922	0.859	0.933	0.798
X-Ray	**0.998**	**0.938**	**0.898**	**0.929**	**0.989**

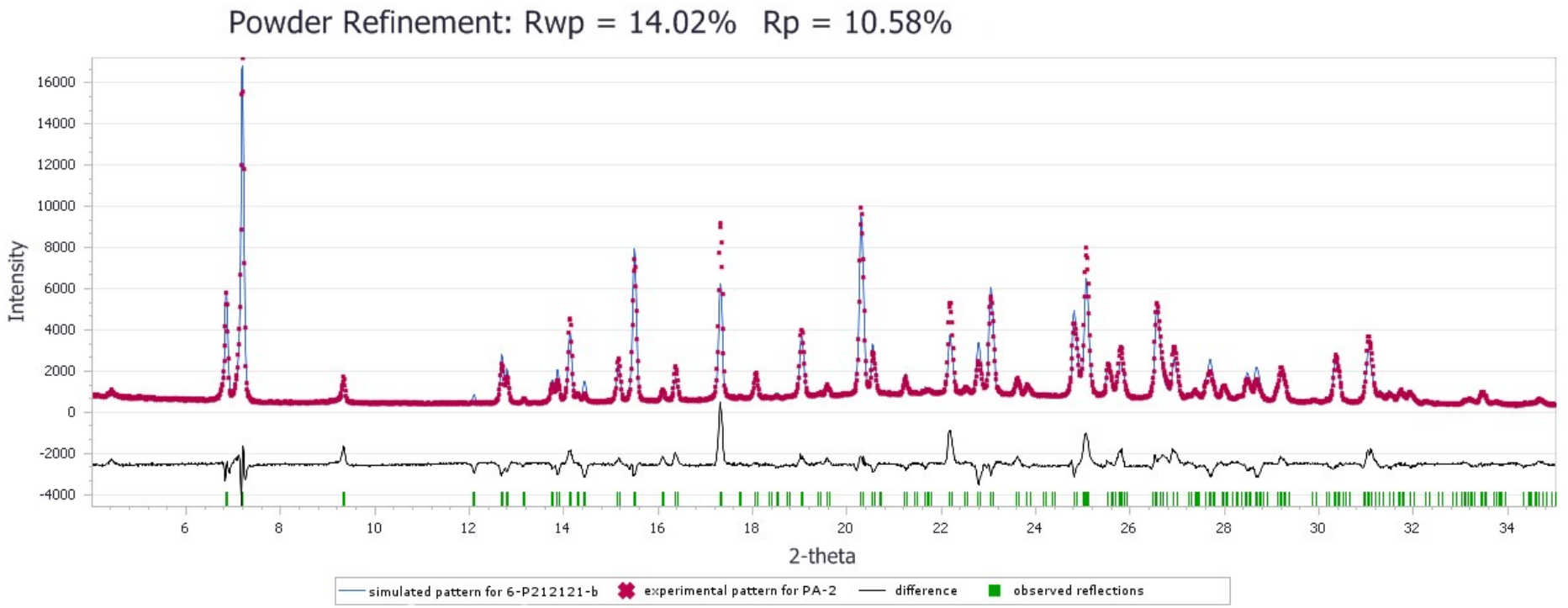

Figure S1. Rietveld refinement results obtained after comparison of experimental powder pattern and the best computationally predicted structure, 6-$P2_12_12_1$-b

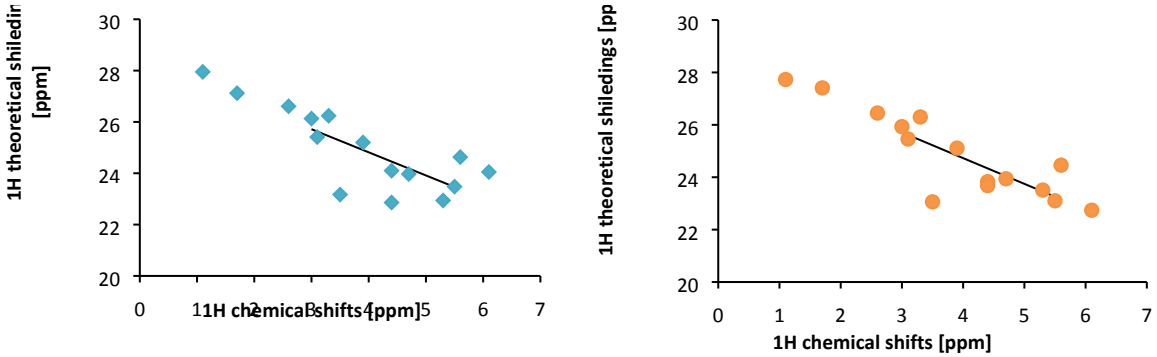

Figure S2. ^{1}H theoretical shieldings for conformers 3-*P*2$_1$2$_1$2$_1$(2) (left) and 7-*P*2$_1$2$_1$2$_1$(2) (right) plotted against experimental chemical shifts. The comparison of experimental ^{1}H NMR chemical shifts and calculated shieldings obtained for structures **3**-*P*2$_1$2$_1$2$_1$(2) and **7**-*P*2$_1$2$_1$2$_1$(1) indicate that ^{1}H NMR data point to the part/parts of the molecule that is/are not in agreement with the true structure. The agreement between theoretical and experimental $\delta_{iso}(^{1}H)$ for **3**-*P*2$_1$2$_1$2$_1$(2) is very poor, mainly due to four points corresponding to H12, H15, H16 and H15' hydrogen atoms, whereas in case of structure **7**-*P*2$_1$2$_1$2$_1$(1) there are only two distinct points, originating from H12 and H15. These hydrogen atoms belong to dihydroxyphenyl rings of both subunits of PA-2, which were varied in conformational search, and therefore, on the basis of the observed NMR discrepancies, it can be concluded that both ϕ and ψ torsion angles in conformer **6** are close to the correct ones, only ψ angle (from lower subunit of PA-2) is correct in **7**, and none is correct in **3**. If we recall the data gathered in Table 1, we will see that **6** and **7** have very similar ψ angle, but not the ϕ one, whereas in **3** both torsions are different than in **6**.

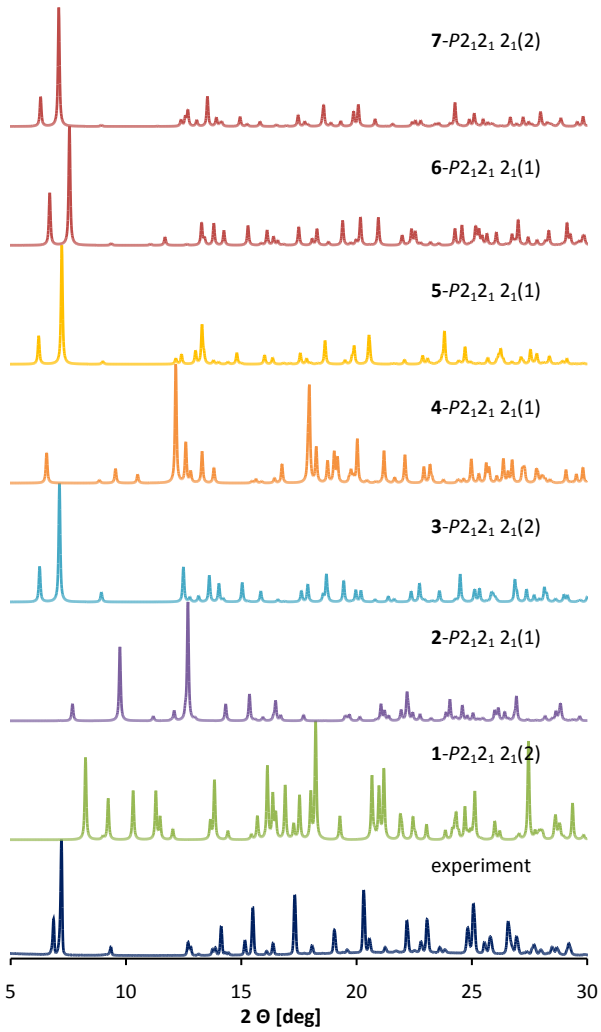

Figure S3. Powder X-Ray diffractograms from experimental measurements and simulations for seven conformers in the $P2_12_12_1$ space group. There is a general similarity between the predicted and experimental PXRD patterns for structures **3**-$P2_12_12_1(2)$, **5**-$P2_12_12_1(1)$, **6**-$P2_12_12_1(1)$ and **7**-$P2_12_12_1(2)$, with still higher match between pairs of {**3**-$P2_12_12_1(2)$, **6**-$P2_12_12_1(1)$} and {**5**-$P2_12_12_1(1)$, **7**-$P2_12_12_1(2)$}. The examination of crystal packing arrangements of these structures is shown in Figure S4.

(a)

(b)

(c)

(d)

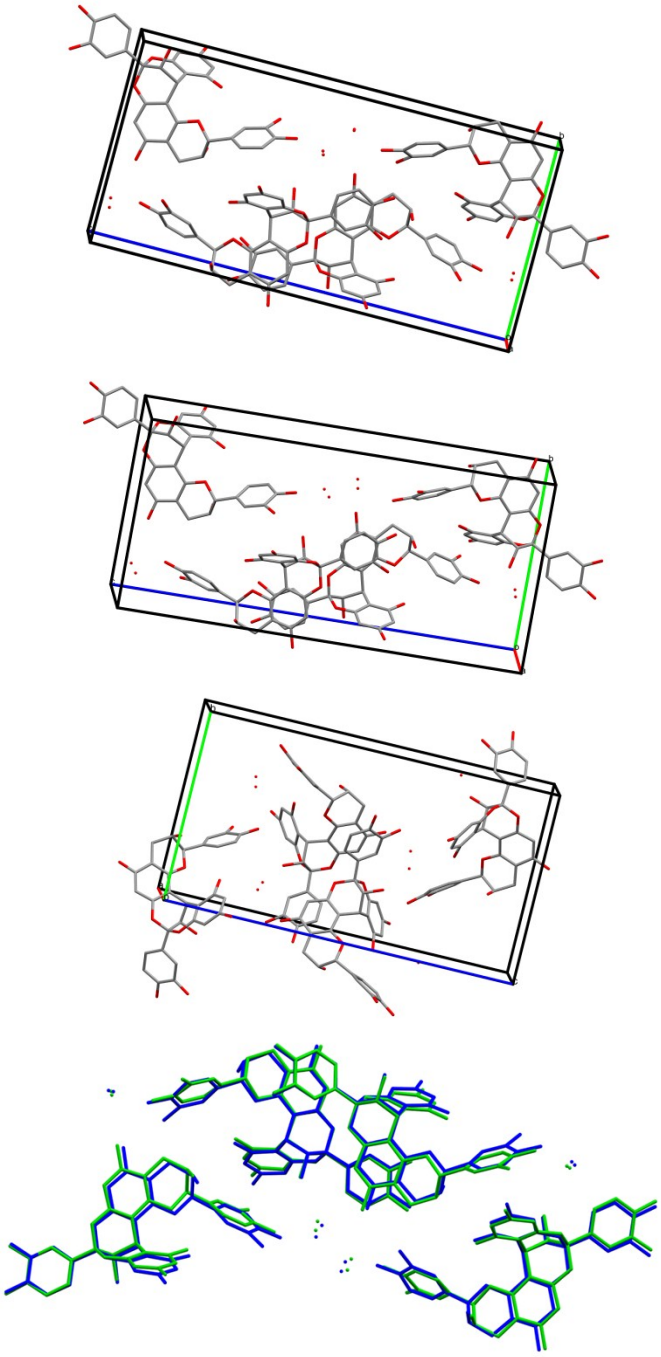

Figure S4. Crystal packing arrangements for **3**-$P2_12_12_1(2)$ (a), **5**-$P2_12_12_1(1)$ (b), and **6**-$P2_12_12_1(1)$ (c), together with the overlay of packing diagrams of structures **3**-$P2_12_12_1(2)$ (blue) and **5**-$P2_12_12_1(1)$ (green) (d). Structures **3**-$P2_12_12_1(2)$ and **5**-$P2_12_12_1(1)$ display very similar packing, with PA-2 molecules interacting by π-π stacking and arranged in almost the same way in respect to each other. The hydrogen bonding network is also similar, but only in structure **3**-$P2_12_12_1(2)$ all hydroxyl groups are hydrogen-bonded, whereas in **5**-$P2_12_12_1(1)$ one hydroxyl group OH-13' does not form such a bond. Likewise, location of water molecules near OH-5' moiety is highly similar. The sole notable difference between these structures, apart from the obvious dihydroxyphenyl ring conformation, is cell volume, which is equal to 2682 and 2856 and 2865 Å^3 for **3**-$P2_12_12_1(2)$ and **5**-$P2_12_12_1(1)$, respectively. The packing arrangement of structure **6**-$P2_12_12_1(1)$ is to some extent different, with two out of three two-fold screw axes differently positioned, but with similar location of water molecules (near OH-5') and π-π stacking interactions of PA-2 molecules. The cell volume of **6**-$P2_12_12_1(1)$ is similar to that of **3**-$P2_12_12_1(2)$ and equal to 2683 Å^3.

The observed similarities and differences between structures **3**-*P*$2_12_12_1$(2), **5**-*P*$2_12_12_1$(1), **6**-*P*$2_12_12_1$(1) and **7**-*P*$2_12_12_1$(2) plainly indicate that cell volume has a notable impact on the PXRD pattern, and that the dihydroxyphenyl ring conformation is less important. Note, however, that the difference in the ϕ and ψ angles values between these structures is usually ca. 180°, which may result in a bit different hydrogen-bonding pattern, but does not change the overall PA-2 shape and therefore the lattice symmetry. It seems that the observed overall similarity for PXRD patterns of these structures is a result of two water molecules location, which for all these conformers are both located near OH-5' group, whereas in structures **1**-*P*$2_12_12_1$(2), **2**-*P*$2_12_12_1$(1) and **4**-*P*$2_12_12_1$(1) they are separated and interact with OH-7 and OH-14'.